FEBS Letters 583 (2009) 2849–2853

FEBS Letters

journal homepage: www.FEBSLetters.org

Impairment of twin-arginine-dependent export by seemingly small alterations of substrate conformation

Carlo Maurer, Sascha Panahandeh, Michael Moser, Matthias Müller *

Institut für Biochemie und Molekularbiologie, ZBMZ, Universität Freiburg, D-79104 Freiburg, Germany

ARTICLE INFO

Article history:
Received 17 June 2009
Revised 20 July 2009
Accepted 20 July 2009
Available online 23 July 2009

Edited by Stuart Ferguson

Keywords:
Twin arginine
Protein secretion
Tat translocase
Quality control

ABSTRACT

The twin-arginine translocation (Tat) machinery is able to transport fully folded proteins across bacterial and thylakoidal membranes. Previous in vivo and in vitro studies indicated that the model Tat substrate TorA–PhoA acquires Tat-competence only if its four cysteines form disulfide bonds. We now show that removal of the last 33 amino acids of PhoA, although not affecting the formation of disulfide bonds, converts TorA–PhoA into a poor Tat substrate. This finding suggests that even incomplete folding of a substrate can interfere with transport by the Tat translocase of *Escherichia coli*.

1. Introduction

Twin-arginine translocation (Tat) denotes a distinct protein transport pathway found in bacteria, archaea, and plant chloroplasts (for a recent review see [1]). Its hallmarks are (i) a consensus motif with an almost invariant pair of arginines in the signal sequences of Tat precursor proteins and (ii) the fact that many of the Tat substrates are transported across membranes in a completely folded conformation. In Gram-negative bacteria like *Escherichia coli*, three functionally distinct membrane proteins named TatA, TatB, and TatC, are required for the twin-arginine-dependent transport across the cytoplasmic membrane. TatB and TatC form a 1:1 complex [2] that assembles into high molecular mass oligomeric structures. A specific function of TatBC is the recognition of the twin-arginine signal peptides. TatA forms homo-multimeric complexes both in vitro and in vivo, which when isolated have the shape of pore-like structures [3]. The actual protein-conducting device of the Tat apparatus has, however, remained elusive. Likewise, the precise mechanism by which the indispensable H^+-motive force is transduced into vectorial protein movement is not understood. Although the Tat machinery can export unfolded protein domains [4,5], Tat substrates, which normally undergo folding in the cytosol prior to export, do not pass through the Tat pathway, if not folded [6–8].

Trimethylamine *N*-oxide reductase (TorA)–PhoA is a model Tat substrate from *E. coli* which was previously shown to be exported in a Tat-dependent manner, provided that its four cysteines were allowed to form dilsulfide bridges under oxidizing conditions [6,7]. Although reduced and therefore presumably unfolded TorA–PhoA nevertheless was found to associate with the Tat translocase of *E. coli* [7,9], its binding to the TatBC receptor site, as revealed by site-specific cross-linking, was perturbed [7] suggesting a kind of a quality control function of TatBC.

Here we have analyzed shortened versions of TorA–PhoA and find that truncation interferes with translocation of oxidized TorA–PhoA. These findings suggest that the Tat machinery scrutinizes its substrates to an extent that even incomplete folding states are recognized.

2. Materials and methods

2.1. Plasmid construction

PCR-based site-specific mutations were introduced into plasmid pET28a-TorA–PhoA [7] using the QuikChange Site-directed Mutagenesis kit system (Stratagene). In order to create a 173 amino acid N-terminal fragment of TorA–PhoA, the two complementary oligonucleotides TorA–PhoA173 for (5′-GCG CTG GGC GTC GAT TAG CAC GAA AAA GAT CAC CCA-3′) and TorA–PhoA173 rev (5′-TGG GTG

Abbreviations: AMS, 4-acetamido-4′-maleimidylstilbene-2,2′-disulfonic acid; INVs, inverted inner membrane vesicles; PK, proteinase K; Tat, twin-arginine translocation; TCA, trichloroacetic acid; TorA, trimethylamine *N*-oxide reductase

* Corresponding author. Fax: +49 761 203 5274.
E-mail address: matthias.mueller@biochemie.uni-freiburg.de (M. Müller).

0014-5793/$36.00
doi:10.1016/j.febslet.2009.07.038

ATC TTT TTC GTG CTA ATC GAC GCC CAG CGC-3′) were used. Analogously, TorA–PhoA269, TorA–PhoA328, and TorA–PhoA466 were constructed using TorA–PhoA269 for (5′-GCA ACC GCC GGT GAA TAG CAG GGA AAA ACG CTG-3′) and TorA–PhoA269 rev (5′-CAG CGT TTT TCC CTG CTA TTC ACC GGC GGT TGC-3′); TorA–PhoA328-for (5′-ACG TAC CAC GGC AAT TAG GAC AAG CCC GCA GTT ACC-3′) and TorA–PhoA328 rev (5′-GGT AAC TGC GGG CTT GTC CTA ATT GCC GTG GTA CGT-3′); TorA–PhoA466 for (5′-CAT ACC GGT AGT CAG TAG CGT ATT GCG GCG TAT GGC-3′) and TorA–PhoA466 rev (5′-GCC ATA CGC CGC AAT ACG CTA CTG ACT ACC GGT ATG-3′). Plasmid pET28aTorA–PhoAΔSP [5] was used as template under the same conditions to obtain non-cleavable TorA–PhoA truncations having Ala40 and 41 each replaced by Leu.

2.2. In vitro reactions

An S-135 was prepared from the *E. coli* strain SL119 [10] and coupled transcription/translation of TorA–PhoA DNAs was

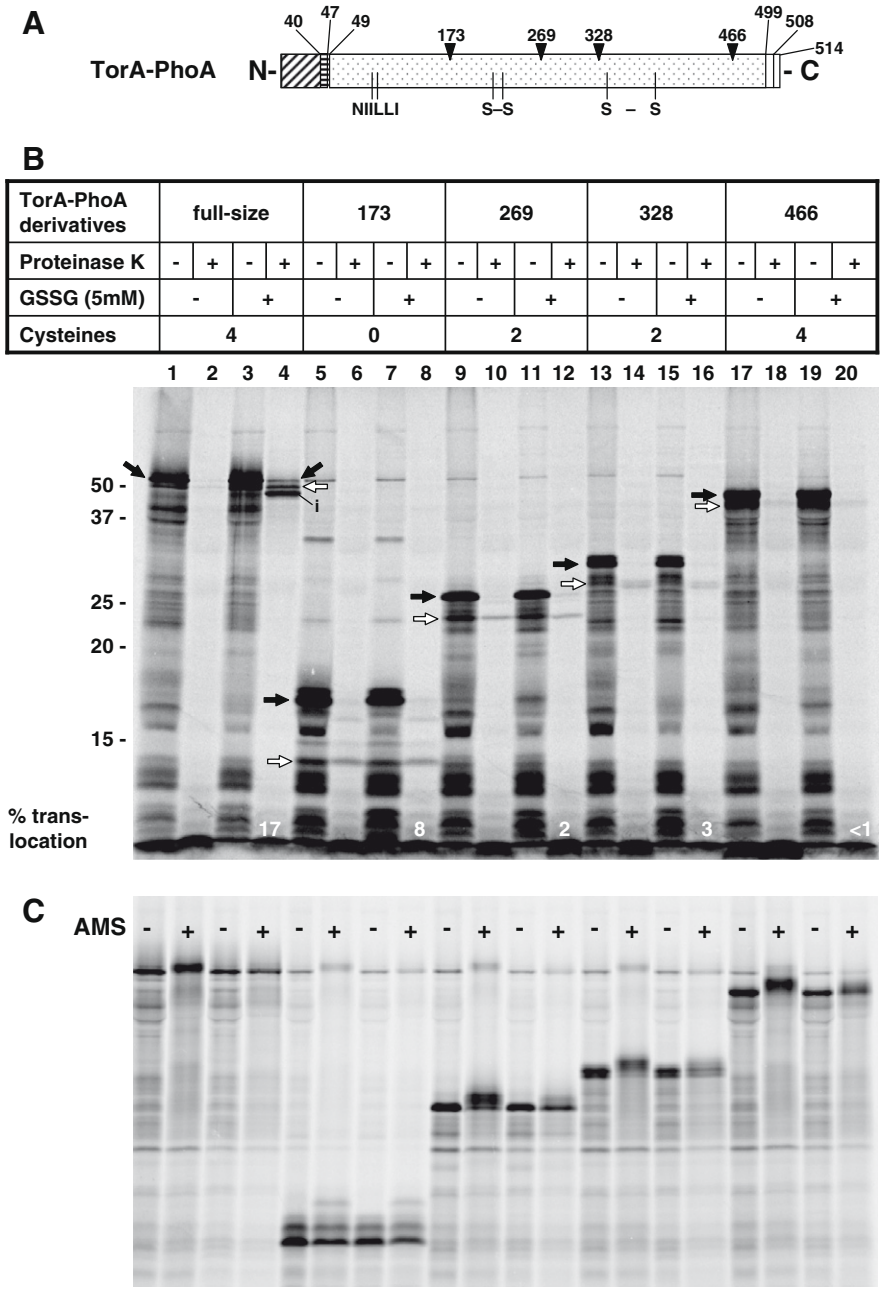

Fig. 1. C-terminal truncation of TorA–PhoA imparts translocation competence to reduced species but interferes with that of a fully oxidized variant. (A) TorA–PhoA consists of the 40 amino acid-long RR-signal sequence of *Escherichia coli* TorA (diagonally hatched area), 7 amino acids derived from mature TorA (horizontally hatched area), two residues introduced by cloning, the mature *E. coli* alkaline phosphatase (stippled area), a nine residue vector-derived linker, and six His residues. The approximate positions of the hydrophobic NIILLI sequence and of the two disulfide bonds are indicated. Black triangles mark the amino acid positions of the truncations. (B) The indicated TorA–PhoA variants were synthesized in vitro in the presence of ^{35}S-labelled Met/Cys under reducing and oxidizing (GSSG) conditions, and are displayed following SDS–PAGE and phosphorimaging (black arrows). White arrows mark the mature, signal sequence-less TorA–PhoA species (as verified below in Fig. 2B). Translocation into INVs prepared from a TatABCD-overproducing *E. coli* strain is visualized by resistance toward proteinase K and was calculated as the percentage of all PK-resistant species relative to the amount of each TorA–PhoA species. (C) As in (B) except that the even numbered samples were treated with AMS instead of PK in the absence of INVs. Full-size forms observed in lanes 5–20 are due to some read-through of the amber stop codon mutants occurring under our in vitro conditions.

performed as described [11]. Inverted inner membrane vesicles (INVs) were prepared according to [11] from the *E. coli* strain AD179 (MC4100 Δ*ompT*) [12]. Tat$^+$-INV were prepared from *E. coli* strain BL21(DE3)pLysS p8737 [13] induced by 1 mM isopropyl thio-β-D-galactopyranoside for the synthesis of TatABC. Transport assays were performed according to [11]. Treatment with 4-acetamido-4′-maleimidylstilbene-2,2′-disulfonic acid (AMS) has been described elsewhere [7].

3. Results

As depicted in Fig. 1A, the *E. coli* model Tat substrate TorA–PhoA is a fusion protein consisting of the RR-signal sequence of TorA and alkaline phosphatase (PhoA). We have synthesized TorA–PhoA in vitro in the presence of inner membrane vesicles (INVs) of *E. coli* (Fig. 1B, lanes 1–4, black arrows). Only when TorA–PhoA was synthesized in the presence of oxidized glutathione (GSSG), were substantial amounts of proteinase K (PK)-resistant species detected (compare lanes 2 and 4). PK-resistance results form the transport of oxidized TorA–PhoA into the protease-inaccessible interior of the membrane vesicles. As previously shown [7], the three PK-resistant species obtained are the precursor (black arrow), the signal sequence-less form (white arrow), and an incompletely protected translocation intermediate (i) of TorA–PhoA. To verify that translocation of TorA–PhoA into INVs correlates with the formation of disulfide bonds, alkylation with AMS was performed (Fig. 1C). When TorA–PhoA is synthesized under reducing conditions, the presence of free thiol groups is indicated by a small increase in molecular mass following alkylation with AMS (lane 2). As proof of principle, a truncated version of TorA–PhoA devoid of

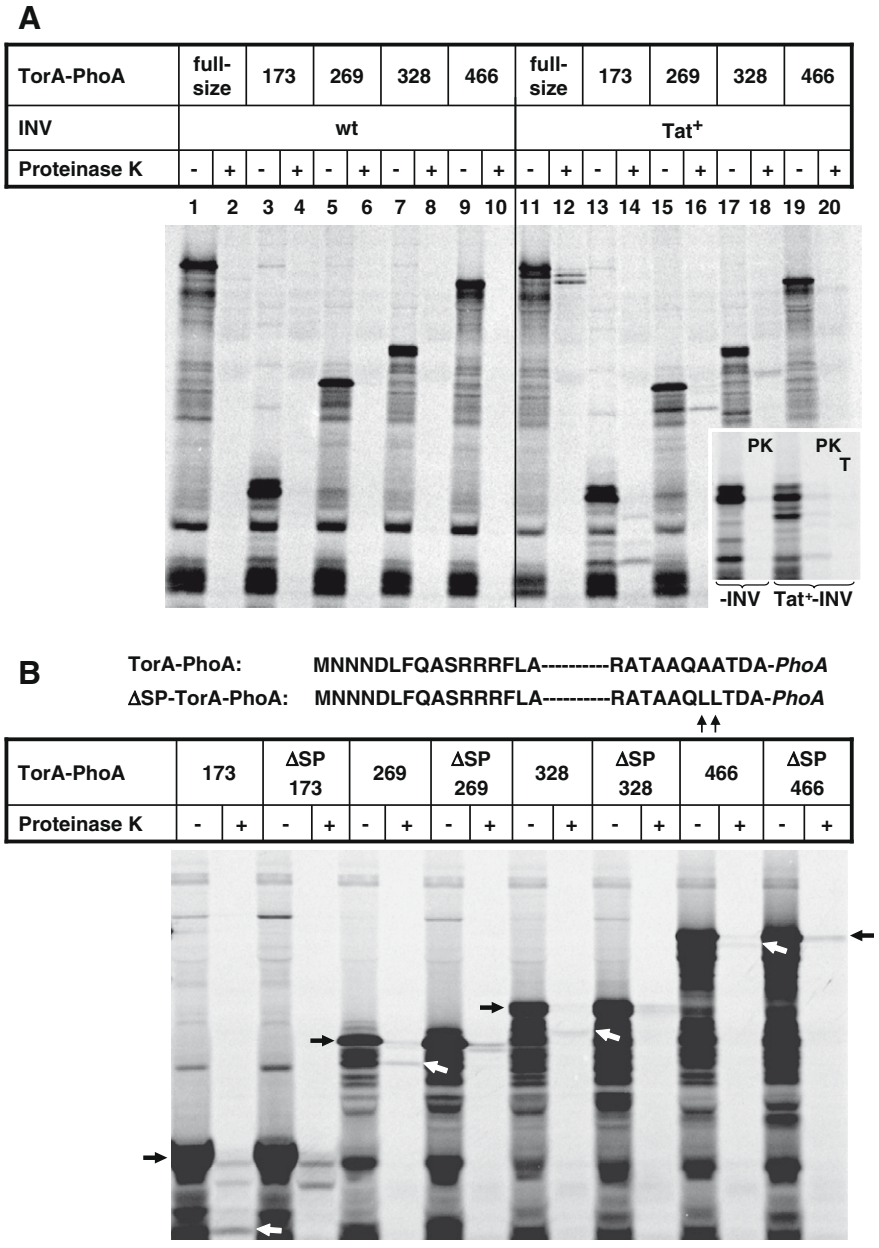

Fig. 2. Translocation of truncated TorA–PhoA variants is Tat-dependent and involves cleavage of the signal sequence. (A) Full-size and truncated forms of TorA–PhoA were synthesized in the presence of INVs prepared from *E. coli* strains expressing *tatABCD* at wild-type (wt) or elevated levels (Tat$^+$). PK-resistance was abolished by disrupting Tat$^+$-INVs by TritonX-100 (T) as depicted for TorA–PhoA(173) in the inset. (B) Black arrows mark the precursors of each TorA–PhoA truncate and white arrows their cleavage products by signal peptidase, as they are each missing from the lanes of the non-cleavable TorA–PhoA variants.

any cysteine, i.e. lacking free thiols, was not modified by AMS (lanes 5–8). Likewise, no modification with AMS was observed when full-length TorA–PhoA was synthesized in the presence of GSSG (lane 4). Therefore under these oxidizing conditions, the four cysteines of PhoA must have formed disulfide bonds thereby allowing TorA–PhoA to adopt a translocation-competent conformation.

We next analyzed the influence of C-terminal truncations on the translocation behaviour of TorA–PhoA. Truncates were obtained by engineering stop codons into the template DNA encoding TorA–PhoA at the positions marked with triangles in Fig. 1A. Unexpectedly, truncation resulted in a gain of translocation-competence under non-oxidizing conditions. Different from full-size TorA–PhoA (Fig. 1B, lanes 1–4), each TorA–PhoA truncate (lanes 5–20, black arrows) yielded PK-resistant species with equal efficiency both in the presence and absence of GSSG (compare lanes 6 and 8, 10 and 12, 18 and 20). A comparison of lanes 10, 14, and 18 between panels B and C of Fig. 1 reveals that those truncates exhibited PK-resistance despite the fact that they were modified with AMS. Thus translocation into the INVs occurred even though disulfide bonds had not formed. The gain of transport-competence under reducing conditions was not due to the concomitant removal of the C-terminal tag (residues 499–514, Fig. 1A), as demonstrated in the Supplemental Fig. 1 depicting comparable translocation efficiencies for TorA–PhoA and its tag-less version.

Surprisingly, an almost complete loss of translocation was observed for the longest truncate TorA–PhoA(466), which lacks only 33 amino acids from the C-terminus of wild-type PhoA (Fig. 1B, compare lanes 4 and 20). This construct possesses all four cysteines of authentic PhoA and therefore forms disulfide bonds under oxidizing conditions, as confirmed by its resistance toward modification with AMS (Fig. 1C, compare lanes 18 and 20). Quantification revealed (Fig. 1B) that the translocation efficiency decreased from 17% for full-size TorA–PhoA to 8% for the smallest truncate and to less than 1% for the longest truncate TorA–PhoA(466). Thus even a relatively minor deletion renders oxidative folding of the PhoA moiety insufficient for Tat translocation.

To examine whether translocation into INVs of the truncated TorA–PhoA proteins in fact occurred via the Tat route, we compared INVs containing wild-type levels of TatABC proteins with those prepared from a TatABCD-overproducing strain. In accordance with previous results [13,14], only the latter vesicles yielded protease-resistant bands of full-size TorA–PhoA (Fig. 2A, lanes 2 and 12), i.e. allowed Tat-specific transport. Likewise for all TorA–PhoA truncates, protease protection was only observed when Tat^+-INV were used indicating that all protease-resistant TorA–PhoA species reflected translocation by the TatABC machinery.

Especially the shorter TorA–PhoA truncates yielded PK-resistant fragments that were seemingly smaller than expected for the mere removal of the signal sequence (Fig. 1B, white arrows). Nevertheless all fragments disappeared when the PK-treatment was performed in the presence of Triton X-100 to disintegrate the INVs (exemplified for the 173 amino acid-long truncate in Fig. 2A, inset, lane T). Hence all these PK-fragments must be membrane-protected forms of TorA–PhoA. In order to identify those small fragments, we examined non-cleavable variants of the TorA–PhoA truncates. These were synthesized from TorA–PhoA DNA templates encoding a mutated signal peptidase cleavage site (ΔSP; cf. top of Fig. 2B). When comparing pairs of cleavable and non-cleavable TorA–PhoA truncates (Fig. 2B), the smallest of the PK-resistant species (white arrows) each was missing from the corresponding ΔSP lane. Thus the bands marked with white arrows in fact are the cleavage products of signal peptidase and therefore originate from a true transport into the membrane vesicles.

Collectively, the TatABC translocase of *E. coli* is obviously able to transport shorter versions of the Tat precursor TorA–PhoA even if compact folding by disulfide bond formation was prevented. Most notably, however, the removal of only 33 amino acids from the authentic C-terminus of PhoA caused an almost complete block of translocation although both disulfide bridges had formed (Fig. 1B, compare lanes 4 and 20). The Tat machinery of *E. coli* thus seems to be able to sense with scrutiny incomplete folding states of its substrates.

4. Discussion

As shown both in vivo and in vitro, full-size TorA–PhoA is only accepted by the Tat machinery of *E. coli* when it is synthesized under oxidizing conditions that lead to disulfide bridge formation within the PhoA moiety (Fig. 1B and [6,7]). In striking contrast, we now find that (i) the formation of disulfide bonds does not any more warrant Tat-dependent translocation when 33 amino acids are missing from the C-terminus, and (ii) C-terminally truncated derivatives of TorA–PhoA can be translocated via the Tat pathway even under reducing conditions, i.e. when no disulfide bonds were formed. The smallest truncate TorA–PhoA(173) is devoid of any cysteinyl residue (Fig. 1A) and the redox state was therefore not expected to exert an influence on its translocation efficiency. Tat translocation proficiency of this small Tat substrate could best be explained by recent findings showing that even unstructured and extended polypeptides are accepted by the Tat machineries of *E. coli* and plant chloroplasts, provided that they are shorter than 100–120 amino acids [4,5]. The reduced translocation efficiency of TorA–PhoA(173) compared to full-size TorA–PhoA could then be due to its length exceeding this translocation cut-off of 100–120 amino acids for extended Tat substrates.

Consistent with the occurrence of the two proximal cysteines of PhoA in TorA–PhoA(269) and TorA–PhoA(328) (cf. Fig. 1A), these truncates form disulfide bonds in the presence of GSSG (Fig. 1C). Since these two thiol groups are, however, only 10 residues apart, their covalent linkage creates only a short loop, which could explain why the translocation efficiencies for the oxidized and reduced forms were virtually non-distinguishable. Totally unexpected was, however, the finding that the longest TorA–PhoA(466) truncate was hardly translocated into INVs even though it contains all four cysteinyl residues of authentic PhoA and as judged by its almost complete resistance to modification by AMS was fully oxidized when synthesized in the presence of GSSG. In this truncate, the two distal cysteines span 50 amino acids of PhoA, of which it is reasonable to believe that they lead to a compaction of the molecular shape upon disulfide bridging [15].

The drastic loss of Tat translocation competence of oxidized TorA–PhoA(466) compared to the full-size precursor must then originate from the removal of the C-terminal 33 amino acids of PhoA deleting one α-helix and the two marginal β-strands of a centrally located ten-stranded β-sheet of authentic PhoA [15]. Two scenarios are conceivable; either destabilization of TorA–PhoA's global structure by the C-terminal deletion causes exposure of some hydrophobic sites and thereby interferes with translocation. Alternatively, incomplete folding of oxidized TorA–PhoA(466) could generate an extended surface area, which was reported to be a critical parameter for Tat-dependent export [5].

Translocation of TorA–PhoA(466) could be compromised by the exposure of hydrophobic sites within mature PhoA, like the hydrophobic peptide NILLII, which Richter et al. demonstrated to effectively block Tat-dependent export of natively unfolded domains [4]. Since this NILLII motif is contained within the first 50 amino acids of PhoA (Fig. 1A), it should, however, be exposed from all shorter TorA–PhoA truncates, especially when they are kept under reducing conditions. Since the shortest TorA–PhoA(173) truncate was the most translocation-proficient construct tested here, we

assume that under all our experimental conditions none of the constructs exposed the NILLII and related hydrophobic patches to an extent that they impeded Tat translocation.

We therefore assume that all reduced and oxidized TorA–PhoA truncates used in this study must have been at least partially folded. The conspicuous translocation incompetence of TorA–PhoA(466) might then most likely be caused by an enlargement of the surface area, which in this instance would originate from a decompaction of the tertiary structure of PhoA following this relatively discrete deletion at the C-terminus of TorA–PhoA.

Acknowledgements

We thank Dorothea Trescher for isolating wt-INVs. This work was supported by Grant LSHG-CT-2004-005257 of the European Union and by the Deutsche Forschungsgemeinschaft (Collaborative Research Centre 746). C.M. was supported by a F.F. Nord-Fellowship from the University of Freiburg.

Appendix A. Supplementary data

Supplementary data associated with this article can be found, in the online version, at doi:10.1016/j.febslet.2009.07.038.

References

[1] Panahandeh, S., Holzapfel, E. and Müller, M. (2009) The twin-arginine translocation pathway in: Bacterial Secreted Proteins (Wooldridge, K., Ed.), pp. 23–43, Caister Academic Press, Norfolk, UK.
[2] Bolhuis, A., Mathers, J.E., Thomas, J.D., Barrett, C.M. and Robinson, C. (2001) TatB and TatC form a functional and structural unit of the twin-arginine translocase from *Escherichia coli*. J. Biol. Chem. 276, 20213–20219.
[3] Gohlke, U., Pullan, L., McDevitt, C.A., Porcelli, I., de Leeuw, E., Palmer, T., Saibil, H.R. and Berks, B.C. (2005) The TatA component of the twin-arginine protein transport system forms channel complexes of variable diameter. Proc. Natl. Acad. Sci. USA 102, 10482–10486.
[4] Richter, S., Lindenstrauss, U., Lucke, C., Bayliss, R. and Brüser, T. (2007) Functional Tat transport of unstructured, small, hydrophilic proteins. J. Biol. Chem. 282, 33257–33264.
[5] Cline, K. and McCaffery, M. (2007) Evidence for a dynamic and transient pathway through the TAT protein transport machinery. EMBO J. 26, 3039–3049.
[6] DeLisa, M.P., Tullman, D. and Georgiou, G. (2003) Folding quality control in the export of proteins by the bacterial twin-arginine translocation pathway. Proc. Natl. Acad. Sci USA 100, 6115–6120.
[7] Panahandeh, S., Maurer, C., Moser, M., DeLisa, M.P. and Müller, M. (2008) Following the Path of a Twin-arginine Precursor along the TatABC Translocase of *Escherichia coli*. J. Biol. Chem. 283, 33267–33275.
[8] Matos, C.F., Robinson, C. and Di Cola, A. (2008) The Tat system proofreads FeS protein substrates and directly initiates the disposal of rejected molecules. EMBO J. 27, 2055–2063.
[9] Richter, S. and Brüser, T. (2005) Targeting of unfolded PhoA to the TAT translocon of *Escherichia coli*. J. Biol. Chem. 280, 42723–42730.
[10] Lesley, S.A., Brow, M.A. and Burgess, R.R. (1991) Use of in vitro protein synthesis from polymerase chain reaction-generated templates to study interaction of *Escherichia coli* transcription factors with core RNA polymerase and for epitope mapping of monoclonal antibodies. J. Biol. Chem. 266, 2632–2638.
[11] Moser, M., Panahandeh, S., Holzapfel, E. and Müller, M. (2007) In vitro analysis of the bacterial twin-arginine-dependent protein export. Methods Mol. Biol. 390, 63–80.
[12] Akiyama, Y. and Ito, K. (1990) SecY protein, a membrane-embedded secretion factor of *E. Coli*, is cleaved by the ompT protease in vitro. Biochem. Biophys. Res. Commun. 167, 711–715.
[13] Alami, M., Trescher, D., Wu, L.F. and Müller, M. (2002) Separate analysis of twin-arginine translocation (Tat)-specific membrane binding and translocation in *Escherichia coli*. J. Biol. Chem. 277, 20499–20503.
[14] Yahr, T.L. and Wickner, W.T. (2001) Functional reconstitution of bacterial Tat translocation in vitro. EMBO J. 20, 2472–2479.
[15] Wang, J., Stieglitz, K.A. and Kantrowitz, E.R. (2005) Metal specificity is correlated with two crucial active site residues in *Escherichia coli alkaline* phosphatase. Biochemistry 44, 8378–8386.